Computer Simulation of an Unsprung Vehicle
Part II

C. E. Goering and W. F. Buchele
MEMBER ASAE MEMBER ASAE

COMPUTATION PROCEDURE

DIAN (DIgital ANalog), a programming system developed by Farris (4), was used for solving the equations in the model. DIAN allows a digital computer to be programmed using analog computer programming techniques. The DIAN program deck is fed into the digital computer to instruct it to simulate an analog computer. Problem "patching" is simulated by means of a coded data deck. One IBM card represents each component of the simulated analog computer. A complete description of DIAN cannot be given here. Readers interested in using the system are referred to a programming guide by Farris and Burkhart (5). Since DIAN solves equations incrementally, the equations must be written in slightly different form than for programming on an analog computer. This is because of the particular incremental form of the inputs and outputs to the DIAN components illustrated in Figs. 7 and 8.

EXPERIMENTAL DATA

As previously mentioned, the prototype was a heavily ballasted tractor. Consequently the following parameters, which were taken from the prototype, are not representative of a normally equipped tractor:

X_{12} = 93.13 in.
Z_{12} = 13.81 in.
Z_{21} = 27.88 in.
X_{11} = 11.15 in.
Z_{11} = 1.60 in.
W_1 = 12,310 lb
I_θ = 46,430 in.-lb-sec^2
I_2 = 1,085 in.-lb-sec^2
H_{11} = 11.26 in.
Θ_{11} = 0.1425 rad
H_{12} = 83.38 in.
Θ_{12} = 0.1859 rad
H_{13} = 31.96 in.
Θ_{13} = 0.4189 rad
D_2 = 3.13 in.
C_2 = 27.5 lb-sec per in.
D_4 = 0.665 in.
C_4 = 8.3 lb-sec per in.
l_{20} = 28.95 in.
μ_4 = 0.037
I_e = 17.0 in.-lb.-sec^2
η = 0.94
N = 93.75 (first gear)
N = 35.40 (fourth gear)
T_m = 5600 lb-in. (maximum)

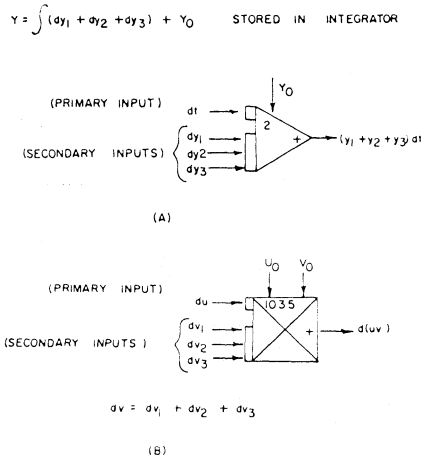

FIG. 7 Schematic representation of an integrator and a function multiplier.

The following empirical functional relationships were obtained for the prototype:

(a) The static force-deflection curve of a rear tire
(b) The static force deflection curve of a front tire
(c) $(\beta_2 - \mu_2) = g\ (TR_2)$
(d) $T_e = T\ (\omega)$
(e) $p = p(t)$

The first two relationships were obtained from tire manufacturers. The third relationship is shown in Fig. 5 and was obtained from data from the National Tillage Machinery Laboratory, Auburn, Ala. The last two relationships were obtained from tests on the prototype tractor.

All variables were given an initial value of zero except the following:

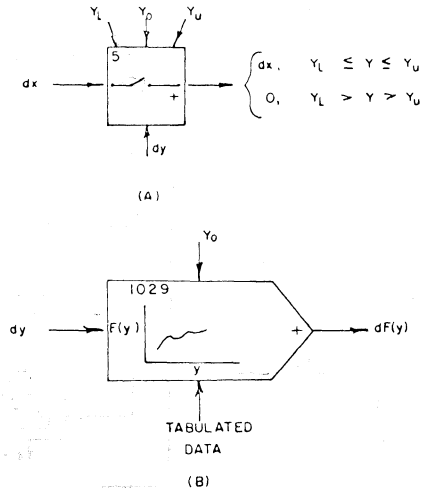

FIG. 8 Schematic representation of a relay and an empirical function generator.

Initial value of $R_{41} = f_{40}$ = 730 lb.
Initial value of $R_{21} = f_{20}$ = 5425 lb
Initial value of $\omega = \omega_o$ = 270 rad/sec

PROGRAMMING THE MODEL

The equations in the model were programmed on an IBM 7074 computer for solution. The flow diagrams given in Figs. 9 through 16 were prepared as a programming aid. These flow diagrams are similar to those which would be used in programming an analog computer.

The flow diagram for the solution of equation [69] (summation of moments on the chassis) is shown in Fig. 9. Nine appropriate input variables (generated elsewhere in the model) are multiplied by appropriate constants and summed. The results, $I_\theta\ d\dot{\theta}$, is divided by I and integrated twice to yield θ.

Equation [70] (summation of forces on the chassis in the z-direction) is programmed on the flow diagram of Fig. 10. Note the nonlinear use of the DIAN integrators for generating product functions, e.g., $\ddot{z}_1\ (\cos\ \theta)\ dt$. A similar flow diagram was used for programming equation [71] (summation of forces on the chassis in the x-direction).

Equations 74 and 75 (kinematics and force relationships on a rear wheel) are programmed on the flow diagram of Fig. 11. For vibration studies, the data stored in empirical function generator (EFG) 1003 could be taken from an actual surface profile. In this problem, s_2 = 0, so EFG 1003 was not used. Data for EFG 1004 were taken from the static force-deflection curve of a rear tire. Relay 200 was used to insure a zero support force on the wheel whenever the tire left the supporting surface. A similar flow diagram was used for programming equations [72] and [73] (kinematics and force relationships on a front wheel).

Fig. 12 illustrates the network for calculation of the rear-wheel speed and the net thrust force. The combination of components 202, 203, 902, 903 and 904 serves to prevent negative wheel speeds. This network transmits only positive increments in wheel speed when it is near zero. Components 68 through 71 make up a reciprocal function generation. Equation [38] (the traction characteristic) is programmed in EFG 1007 in the form of discrete

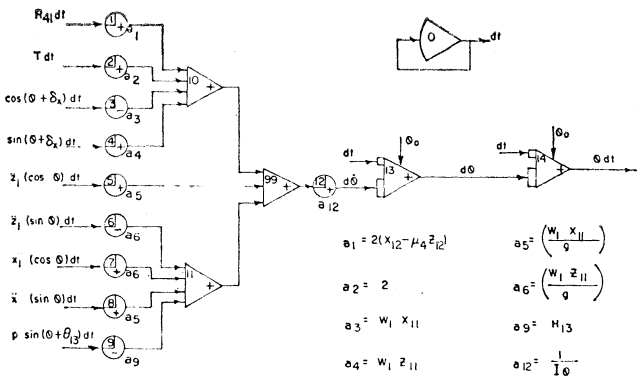

FIG. 9 Flow diagram for the generation of θ.

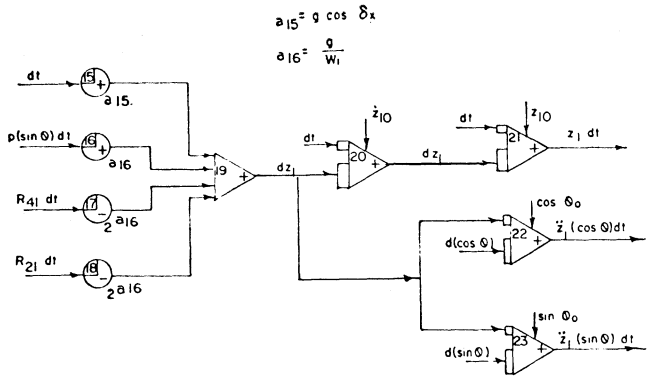

FIG. 10 Flow diagram for the generation of z_1.

data points taken from the traction coefficient vs. travel reduction curve. Components 1008 and 73 represent the programming of equation [70] (force relationships on a rear wheel). The differential, dR_{21}, was not available anywhere in the program for an input to component 1008. The differential, df_2, from EFG 1004 (Fig. 11) was used instead. That is, the effect of damping on the thrust force was neglected.

Fig. 13 shows the flow diagram for generating functions of p. Although in this problem p was known as a function of time, a relationship between p and any other variable could also be used. In the case of a speed-dependent drawbar load, for example, discrete data points of p vs $\dot{x}_2$ could be used as data for EFG 1009, and $d\dot{x}_2$ could replace dt as the input.

Equations [41] through [44] and [52] (the mathematical description of the power train) were used in preparing the flow diagram of Fig. 14, the complete explanation of which is too long to give here. Interested readers are referred to the thesis by Goering (6) for a detailed explanation. The network was designed to receive as inputs the variables required by component 81 and to compute Tdt as an output variable from component 98. The torque-speed relationship of the engine was stored in EFG 1013. The clutch engagement pattern was specified via EFG 1014.

Other flow diagrams (not shown) were prepared for generating trigonometric functions of θ and for programming equation [76] (kinematic relationship for generating an input to Fig. 12).

The complete mathematical model for backward tipping was designated model A. Two other models, B and C, were also devised. In model B the train simulator of Fig. 14 was replaced by the components of Fig. 15. Consequently, an empirical T vs t relationship was required for model B. Model C was derived from model B by replacing Fig. 12 with Fig. 16. Thus in model C, an empirical $\dot{\phi}_2$ vs t relationship was required. Although models B and C required test data from a prototype, they were useful in checking out subsections of the mathematical model.

Results

Clutch Tests

Model A was used to study the behavior of a tractor (without drawbar load) after sudden clutch engagement. The clutch engagement function, $T_m = T(t)$, was assumed to be piecewise linear. Slippage torque T_m was assumed to increase linearly from zero to 5600 lb-in at $t = 0.15$ sec and thereafter remain constant. The value, $t = 0.15$ sec, was chosen because experimental tests revealed that the operator could engage the clutch that quickly. Model A performed satisfactorily for $0 \leq t \leq 0.3$ sec, at which point the engine simulator began erratic behavior. The time, $t = 0.3$ sec, corresponded to the time when the clutch ceased slipping, and, therefore, the time at which the relays of Fig. 14 were actuated. After several unsuccessful attempts to correct the difficulty, Model A was abandoned.

Model B required a torque-time relationship for programming into EFG 1013 (Fig. 15). The torque curve of Fig. 17, which was derived from experimental measurements of rear-axle torque, served as the required relationship. The prototype behavior predicted by model B is shown in Figs. 17 through 20. As shown in Fig. 18, the predicted chassis tip angle increased to 0.295 radians (16.9 deg) and then decreased to zero. Thus model B predicted some tipping but not complete overturning. Fig. 19 illustrates the predicted height of rise of the front wheels vs the for-

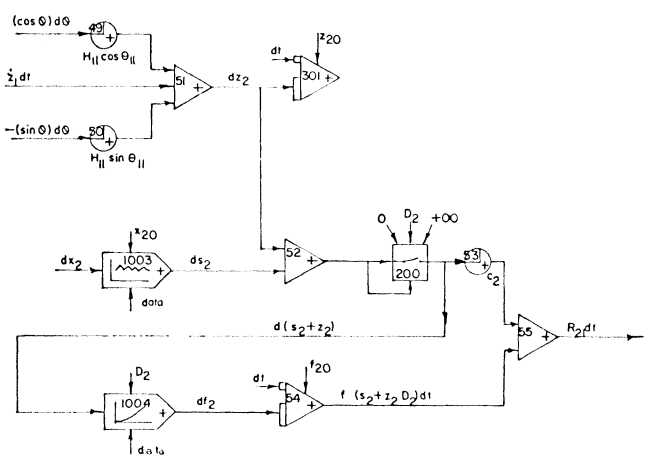

FIG. 11 Flow diagram for the generation of $R_{21}dt$.

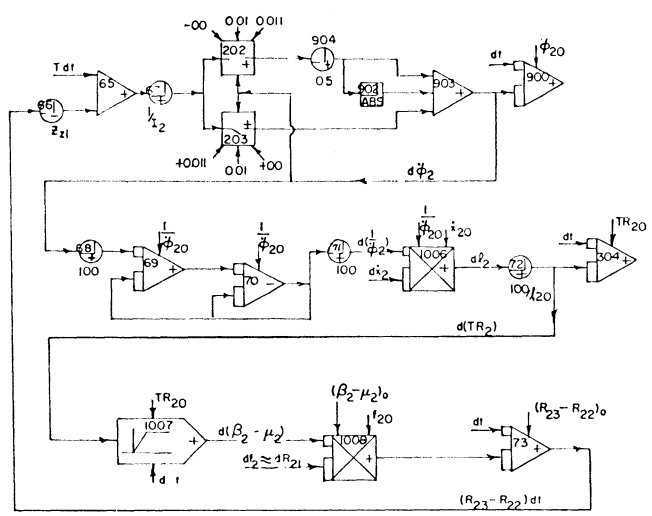

FIG. 12 Flow diagram for the generation of rear-wheel speed and thrust force.

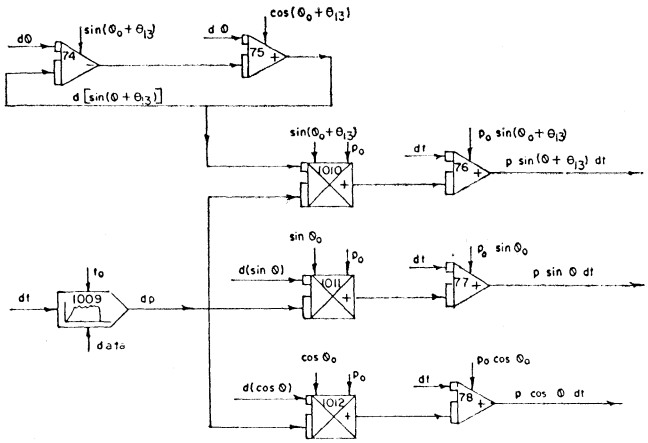

FIG. 13 Flow diagram for the generation of functions of p.

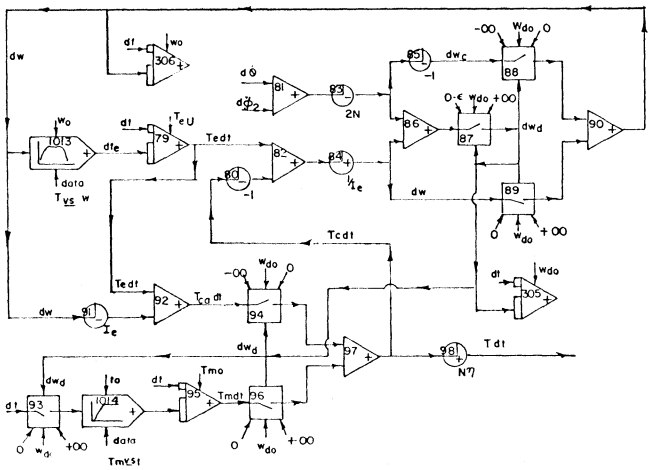

FIG. 14 Flow diagram for simulation of the tractor engine and power train.

ward travel of the prototype. This curve was prepared to determine how nearly the tractor-tipping behavior approached fixed axis rotation about the rear axle. In this case, the forward travel of the tractor was so great that the predicted tipping did not remotely resemble fixed-axis rotation.

Fig. 20 shows the vertical displacement of the rear axles at any time. The variable z_2 is positive downward. Thus the model predicted sinkage of the rear axle as the chassis tipped and vertical oscillation of the rear axle throughout the run.

The travel-reduction curve predicted by model B is shown in Fig. 17. There is a similarity between the travel reduction curve and the torque curve. For values of travel reduction less than 16 percent, the travel reduction was directly proportional to the coefficient of traction (Fig. 5). Thus, according to Fig. 17, the travel reduction and the traction coefficient varied almost directly with the torque the wheels were required to transmit. Since the rear axle oscillated vertically, the rear-wheel support force also oscillated and this explains the oscillations in the travel reduction curve of Fig. 17.

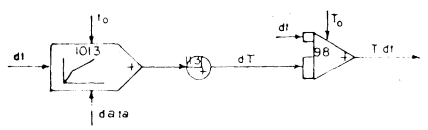

FIG. 15 Alternate flow diagram for generation of T dt.

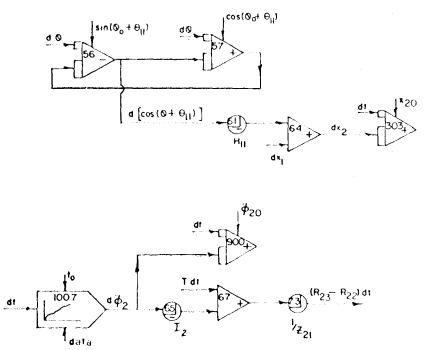

FIG. 16 Alternate flow diagrams for generation of rear wheel translational and rotational speeds and net thrust.

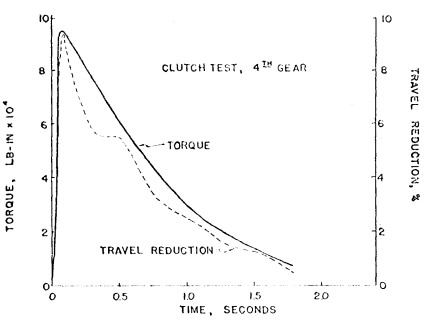

FIG. 17 Empirical torque vs. time curve and calculated travel reduction vs. time curve.

Drawbar Tests

Fig. 21 shows the torque-time curve used in model B for predicting the prototype behavior under load. Fig. 22 shows the p vs t relationship used in the model. In both Figs. 21 and 22 the oscillatory solid curves were obtained experimentally, but the smooth dashed curves were programmed into the model. Figs. 23 and 24 illustrate the predicted behavior of the prototype. Fig. 23 shows that the prototype can move for a long time without overturning, even though the chassis is tipped enough to raise the front wheels off the ground. Fig. 24 illustrates sinking of the rear axles and vertical oscillation of the rear axles throughout the run.

Model C was used in predicting the prototype behavior for both the clutch and the drawbar tests. In model C, the traction-slip curve for the supporting surface was not needed. Instead an experimental relationship between rear-wheel speed and time was required for programming into EFG 1007, Fig. 16. The predictions obtained from model C were in all cases similar to those obtained through use of model B.

Computation Time

The digital computer was slower in solving the model equations than was originally anticipated. The reason was that components in DIAN are serviced serially rather than simultaneously, as on an analog computer. The speed of computation varied approximately linearly with the number of components in the DIAN model, and with the range of t. The computation time varied in-

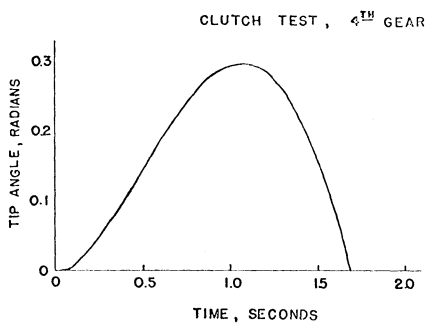

FIG. 18 Calculated curve of tip angle vs. time.

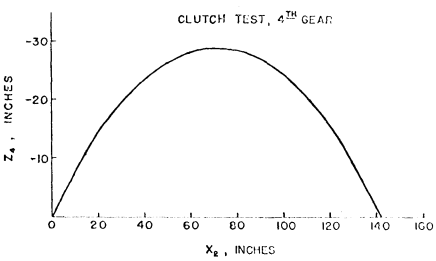

FIG. 19 Calculated curve of z_4 vs. x_2.

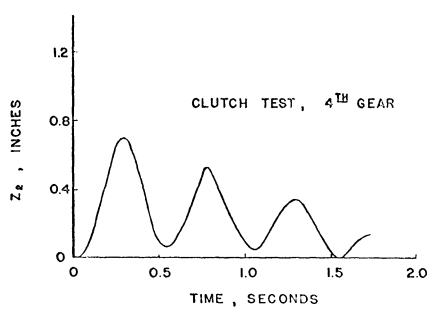

FIG. 20 Calculated curve of z_2 vs. time.

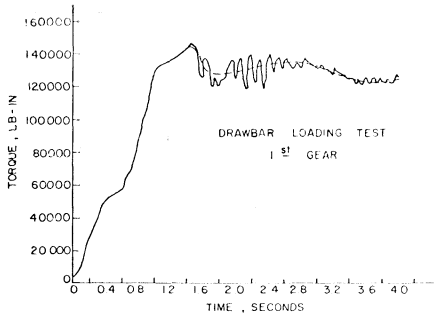

FIG. 21 Empirical curve of torque vs. time.

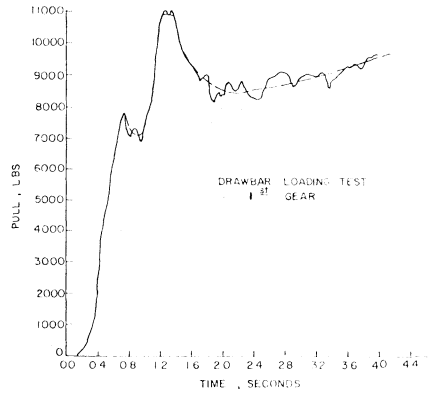

FIG. 22 Empirical curve of p vs. time.

versely with *dt,* the increment in the independent variable.

For the clutch test, which had a range $0 \leq t \leq 1.7$ sec, the computation time for model B was 12 min. This time was achieved only after careful selection of a set of IVGs (independent variable generators). For the drawbar test, the problem range was $0 \leq t \leq 4.0$ sec. It was necessary to select a less efficient set of IVGs for this problem, and the solution of the equations in model B required 45 min. The quantity $1/\dot{\phi}_2$ governed the selection of IVGs. It was necessary to keep *dt* very small whenever low wheel speeds caused $1/\dot{\phi}_2$ to be very large. Since the rear wheel speed increased slowly in the drawbar test, an inefficient set of IVGs had to be used.

Summary and Conclusions

Actual backward overturning and large-amplitude vibration were beyond the scope of the previous investigations into the mechanics of upsprung wheel tractors. Thus the primary objectives of this study was to establish a mathematical model capable of predicting either large-amplitude vibration or backward overturning of an unsprung wheel tractor. Other objectives were to find a means of solving the set of nonlinear differential equations that constituted the model and to check the prediction accuracy of the model through measurements on a prototype. This paper reported on the work involved in meeting the first two objectives.

The mathematical model included equations derived from kinematics and kinetics. Certain empirical functional relationships were also used in the model. Several simplifying assumptions were made prior to derivation of the model. The most restrictive was the assumption of plane motion.

The model was used to predict backward tipping of a prototype (**a**) when no drawbar load was attached but the clutch was suddenly engaged and (**b**) when a heavy drawbar load was attached but the clutch was engaged more slowly. In both cases, the supporting surface was level concrete and the tractor started from rest.

DIAN, a new programming technique, was used in programming the equations in the model. With DIAN, a digital computer is programmed using analog computer programming techniques.

Three mathematical models were devised. Model A, the most extensive model, included an engine simulator. Model B was derived from model A by replacing the engine simulator with torque-time data. Model C was derived from model B by replacing the thrust calculator with empirical wheel speed *vs* time data.

Values for the model parameters were taken from a heavily ballasted John Deere 3010 tractor. Certain empirical function relationships were also obtained from this tractor.

Difficulties with model A caused its abandonment. Model B predicted that, for the conditions specified, the chassis would tip to 16.9 deg and then fall back to 0 deg after rapid engagement of the clutch. The model predicted that the rear axles would sink down and then oscillate vertically throughout the run. The travel reduction (and traction coefficient) was predicted to vary directly with the rear-axle torque, except that the vertical oscillations of the rear axle caused oscillations in the travel-reduction curve. The prototype behavior was predicted to be much different than fixed-axis rotation about the rear axle.

For slower startup under heavy drawbar load, model B predicted that the chassis would not overturn, but the front wheels would be carried above the ground for an appreciable length of time.

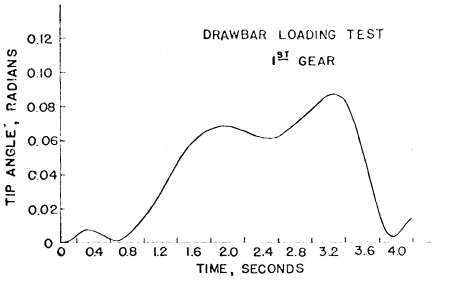

FIG. 23 Calculated curve of tip angle vs. time.

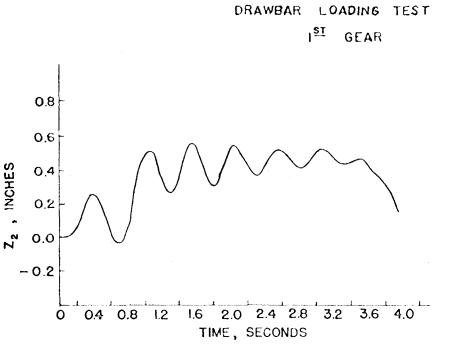

FIG. 24 Calculated curve of z_2 vs. time.

In all cases, predictions from model C were similar to those from model B.

The following conclusions were drawn from this study:

1 Mathematical model A, as presently constructed, could not be solved on the digital computer.

2 The DIAN computation system provided a suitable but relatively slow method of solving the equations in models B and C.

3 The tipping behavior of the tractor was quite different from fixed axis rotation about the rear axle.

4 After sudden clutch engagement, the travel reduction (and traction coefficient) varied almost linearly with rear-axle torque, except that vertical oscillations of the rear axle caused oscillations in the travel-reduction curve.